Photogrammetric Measurements of an EH-60L Brownout Cloud

Oliver D. Wong, Research Scientist
oliver.d.wong@us.army.mil

Philip E. Tanner, Research Scientist
philip.e.tanner@us.army.mil

U.S. Army Joint Research Program Office, Aeroflightdynamics Directorate
NASA Langley Research Center, Hampton, VA 23681

Abstract

There is a critical lack of quantitative data regarding the mechanism of brownout cloud formation. Recognizing this, tests were conducted during the Air Force Research Lab 3D-LZ Brownout Test at the US Army Yuma Proving Ground. Photogrammetry was utilized during two rounds of flight tests with an instrumented EH-60L Black Hawk to determine if this technique could quantitatively measure the formation and evolution of a brownout cloud. Specific areas of interest include the location, size, and average convective velocity of the cloud, along with the characteristics of any defined structures within it. Following the first flight test, photogrammetric data were validated through comparison with onboard vehicle data. Lessons learned from this test were applied to the development of an improved photogrammetry system. A second flight test, utilizing the improved system, demonstrated that obtaining quantitative measurements of the brownout cloud are possible. Results from these measurements are presented in the paper. Flow visualization with chalk dust seeding was also tested. It was observed that pickup forces of the brownout cloud appear to be very low. Overall, these tests demonstrate the viability of photogrammetry as a means for quantifying brownout cloud formation and evolution.

Introduction

Helicopters operating in arid and dusty environments, notably the current theaters in Iraq and Afghanistan, are susceptible to a dangerous condition known as brownout. Brownout occurs when dust and debris are loosened by the high velocity of induced flow near the ground and entrained by the downwash of the helicopter, resulting in the aircraft becoming enveloped in a large cloud of dust[1, 2, 3]. This causes a degraded visual environment (DVE) for the pilot, blinding the pilot and can lead to a loss of situational awareness[4]. This problem presents itself most prominently at altitudes below 50 ft as the helicopter is approaching or departing the landing zone (LZ)[5, 6]. The DVE causes the pilot to lose all visual references to the LZ, and this can induce a dangerous sideward or rearward drift during takeoff or touchdown, which most aircraft cannot safely handle[7]. A similar phenomenon can also present itself in other environments, such as whiteout in Arctic conditions or with water spray in maritime environments[8].

Little is known about the actual mechanics of brownout and the downwash-induced cloud that results[8]. It has been observed that the surface and flight conditions greatly affect the onset of brownout[1], as the composition of the soil is known to contribute to the concentration and size of the brownout cloud[7]. A number of helicopter configuration parameters appear to significantly influence an aircraft's brownout performance. Some of these parameters are configuration (i.e. single main rotor, tandem or tiltrotor), disc loading, blade geometry, radius, twist, root cutout, tip shape, number of blades, rotor RPM, and fuselage shape[1, 9].

The shape of the brownout cloud also seems to be highly influenced by the flight path characteristics of the helicopter as the dust cloud is forming[3]. An example of brownout is shown in Figure 1. In this image, the EH-60L used for this testing is entering into a brownout cloud.

Figure 1. View of an EH-60L entering a brownout cloud

Brownout is a costly phenomenon for all branches of the military, as demonstrated by its status as a joint effort of the Office of the Secretary of Defense[10]. Army pilots have stated that "returning home to land in a dangerous dust cloud is the most frightening part of the day" and the "highest-difficulty maneuver in Army aviation[11]." Helicopters operating in sandy environments have considerably shorter lifetimes of engines, rotor blades, and other components exposed to the erosive downwash[12, 13], as evidenced by the Navy losing a "significant number" of engines due to brownout in 2006[14]. Brownout also limits multiple-aircraft

Presented at the American Helicopter Society 66th Annual Forum, Phoenix AZ, 11-13 May 2010.

operations, greatly reducing the operational tempo, and signals the presence of a helicopter for potential hostile activities[8]. Estimates put the monetary cost of the equipment damage and pilot risk due to brownout at $60 million per year for the US Army alone[15], and $100 million per year for all branches of the military[16].

Interest in brownout has recently increased within the rotorcraft community. This has resulted in a large number of experimental and computational studies[17-22]. Even with these studies, the fundamental physics are not yet well understood. Simulations and modeling of the brownout cloud are still being developed and validated. Validating the simulations has been slowed by a lack of experimental data, especially at full-scale and in relevant environments.

In the research presented herein, photogrammetry was used to obtain quantitative data on the formation and evolution of a brownout cloud formed by an instrumented EH-60L Black Hawk. This paper presents analyses of a subset of the overall data collected. Specific areas of interest include the formation and evolution of the cloud and of any defined fluid structures existing within it. Use of the instrumented vehicle 1) permits validation of the photogrammetric data, and 2) adds vehicle state data to the brownout cloud data to create a more complete dataset for brownout cloud prediction validation.

Photogrammetry

Photogrammetry is a measurement technique that uses photography in determining the two-dimensional or three-dimensional coordinates of an object of interest[23]. For the three-dimensional coordinates of an object to be obtained, multiple photographs of an object are taken from different perspectives. For each photograph, a ray from the camera to a point on the object of interest can be determined, based on the camera sensor size and focal length of the lens used. Through triangulation, these rays from each photograph are intersected. Given at least one known distance in the photographs and a user-defined coordinate system, the three-dimensional coordinates of the points on the object can be found[24].

Photogrammetry, first developed to examine topography[23], is commonly used in architecture, archaeology, engineering and accident reconstruction. Some of the common uses in aerospace engineering include model and equipment positioning, parachute canopy measurements[25], model deformation and rotor blade deformation and position measurements[26, 27]. The photogrammetry in these applications typically uses well-defined targets to automate the data reduction process.

This work presents a new application of photogrammetry in the examination of the brownout cloud. Since a brownout dust cloud does not have well-defined targets, the data reduction process here is fundamentally different. The use of photogrammetry without well-defined targets is not unprecedented, however. Since the early 1950's, photogrammetry has been used to study weather clouds. It allows researchers to make dimensional measurements of clouds and to determine their growth rates[28]. More recently, in 2003, a team of researchers used a three-camera technique for a cloud study in Arizona and successfully implemented an automatic image processing technique[29].

Experimental Setup

The flight testing occurred at the Oasis Landing Zone (LZ), which is located in a remote section in the northern-most part of the US Army Yuma Proving Ground (YPG). A view of the LZ from the roof of the ground test complex looking north can be seen in Figure 2, with Lane 1 in the foreground and the various obstacles in the LZ clearly visible.

Figure 2. View of Oasis LZ, looking north from the ground test complex

Experimental Setup - Round One

For the first round of flight tests, occurring in August 2009, a stereo camera configuration was used to gather the images of the brownout cloud. A schematic of the LZ and camera positions, with indicated fields of view, is shown in Figure 3. Note that north is in the direction of –y. The LZ consists of seven lanes of varying widths, all running east to west. Lanes 1, 3, 5, and 7 (the green lanes) are the ones through which the aircraft travels. The remaining lanes contain a variety of obstacles, such as telephone poles, wires, small buildings and old vehicles, used for testing the detection capability of aircraft onboard sensors. The sand at the LZ was extremely fine, similar to talcum powder, and was tilled by a tractor-pulled disc harrow on the day before testing to break up any crust formed by precipitation. The tilled portion of the LZ was approximately 300 ft long and 945 ft wide.

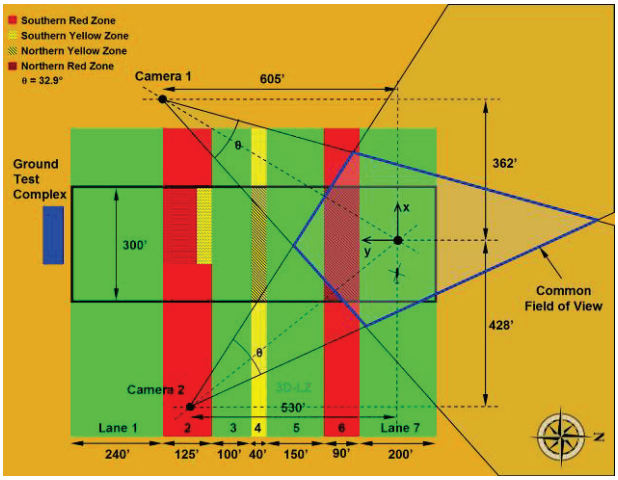

Figure 3. Schematic of Oasis LZ, round one

The photogrammetry equipment consisted of two 2.0 megapixel machine-vision cameras powered by a small gasoline generator. Each camera was sealed in an environmental housing with protective sunshade, mounted on a heavy duty tripod and gearhead, and secured by 50 lb shot bags. Each camera was also fitted with a 20mm lens, resulting in a 32.9° field of view. The setup is shown in Figure 4. The cameras were connected via military-grade optical fiber to a workstation located in the ground test complex just outside the perimeter of the LZ. The workstation was used to control image capture and time-stamp each image with its appropriate GPS time. The cameras were triggered at 15 Hz.


Figure 4. Camera setup, round one

Laboratory calibration before the flight tests was used to characterize each camera and lens combination. The focal length, digitizing scale, principal point, and lens distortion constants were measured using a 2D dot card. Approximately 12 images of the dot card, captured from several orientations and rotations, were used to compute the necessary parameters for each camera and lens combination.

The flight testing occurred for about 1.5 hours, with a total of six events through Lane 7. There was sufficient time between events to allow the brownout cloud to clear before the next pass. The majority of events were an approach to touchdown and takeoff. An image from a typical event, during approach before the aircraft is completely engulfed in the brownout cloud, is shown in Figure 5, while Figure 6 shows the aircraft exiting the cloud.


Figure 5. EH-60L approach to touchdown in Lane 7


Figure 6. EH-60L takeoff after touchdown in Lane 7

Experimental Setup - Round Two

A second round of flight tests was conducted at Oasis LZ in late September 2009 after the previous round showed promising results. A similar test plan as before was followed. Experience gained during the first round of testing was used to develop a new photogrammetry system which was a significant improvement over the system used during the first round of tests in August. The new system consisted of six 15.1 megapixel digital SLR cameras placed evenly about an arc of 75° approximately 550 ft north of the landing zone, as shown in Figure 7. This increase, both in the number and resolution of the cameras, was done to capture more detail of the brownout cloud and to enable easier identification of common features within the cloud.

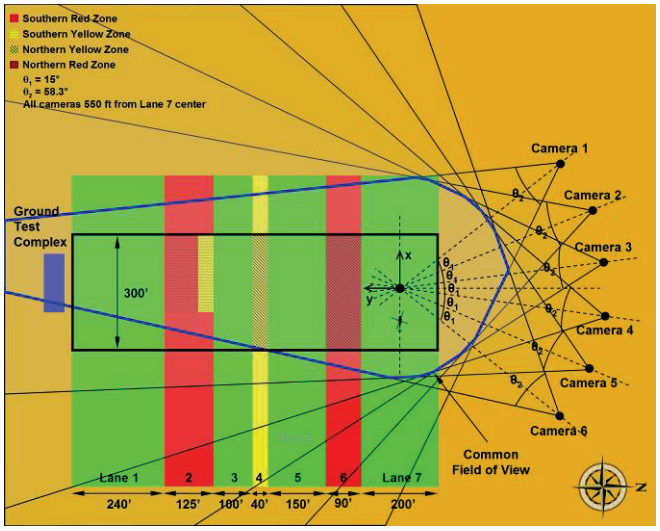

Figure 7. Schematic of Oasis LZ, round two

Each camera was fitted with a 20mm lens, resulting in a 58.3° field of view. The cameras captured the images onto on-board memory. All of the cameras were simultaneously triggered at 3Hz, and each image was stamped with GPS time. For protection from the dust and sun, each camera was wrapped in a plastic rain sleeve and placed under a repositionable umbrella, as shown in Figure 8.


Figure 8. Camera setup, round two

An improved camera calibration process was used as well. This took advantage of a large-scale three-dimensional calibration pattern with retro-reflective targets in a high-bay area at NASA Langley Research Center (LaRC). Approximately twenty photographs were taken with each camera system of the calibration grid at a variety of locations, heights, and camera rotations. An example of this is shown in Figure 9.


Figure 9. Sample level calibration image from second photogrammetry setup

In an attempt to help visualize the pickup mechanism of the brownout cloud, colored chalk was spread in wide lines across Lane 7. Two-hundred-twenty pounds each of red, blue and yellow chalk were manufactured to match the physical flow characteristics to those of the particulate at Oasis LZ. For the first day of the second round of tests, the chalk was poured as-is in approximately six-inch wide lines laterally across the lane. Three lines were made, with a yellow line 100 ft forward (west) of the centerline, a blue line on the centerline, and a red line 100 ft aft (east) of the centerline. On the final day of flight testing, the chalk was mixed with sand from the LZ to better resemble its actual physical properties. The mixture was then poured over the existing lines from the previous day's test and spread to a width of approximately two feet. An additional blue line was added 200 ft aft (east) of the centerline.

Photogrammetry Validation

Validation of the photogrammetry was performed to ensure that accurate quantitative measurements of the brownout cloud could be obtained. Two methods were used to validate the photogrammetry. The first method compared photogrammetric and conventional measurements of the length of the obstacles in the LZ, as well as the distances between traffic cones temporarily placed in the LZ. The differences between measurements were then used to estimate an error bound. The second method compared the onboard flight track data from the inertial measurement unit (IMU), embedded GPS/INS (EGI) and radar altimeter to the vehicle trajectory measured by photogrammetry. Both of these validation techniques were done for each round of flight tests.

Photogrammetry Validation - Round One

The first method of validating the photogrammetry technique involved comparing measurements made of various objects in the LZ to physical measurements taken onsite. These objects included the traffic cones, telephone poles, and stationary vehicles. Orange traffic cones were placed at arbitrary distances in the positive and negative X and Y directions, as well as at the origin. The telephone poles were approximately 34 ft tall. The comparison of

these different lengths are given in Table 1, and it can be seen that they are in fairly good agreement with one another, as the largest difference in magnitude is an error of 4.38%.

Table 1. Measured and calculated distances, round one

Object	Measured (ft)	Photogrammetry (ft)	Delta
LZ_0[a] to +X Cone	135.5	139.7	3.09%
LZ_0[a] to -X Cone	115	120.0	4.38%
LZ_0[a] to +Y Cone	183	185.0	1.07%
LZ_0[a] to -Y Cone	158.5	156.6	-1.23%
Pole 1 Height	34*	33.4	-1.80%
Pole 2 Height	34*	32.7	-3.75%
UH-1 Tail Height	9.5	9.5	0.24%

[a]Center of Lane 7 in Oasis LZ
*Approximate height

The second validation involved comparison of the vehicle position from photogrammetric measurements and on-board vehicle position measurements during a taxi pass of the Oasis LZ. For this pass, the aircraft was traveling approximately 20 kts. Figure 10 displays the longitudinal position versus the lateral position of the aircraft during the taxi pass through Lane 7 is shown in Figure 10. The longitudinal position versus the altitude of the aircraft for the same pass is shown in Figure 11. Comparison of the photogrammetry data and the measured vehicle track shows good correlation. A direct comparison of the two data sets at the same time stamp was not possible due to a GPS timing offset. The offset was found to be induced during the initial GPS startup process and was rectified for the second round of flight tests.

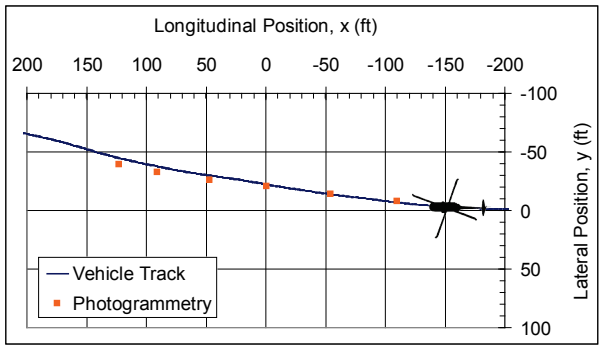

Figure 10. Longitudinal versus lateral position

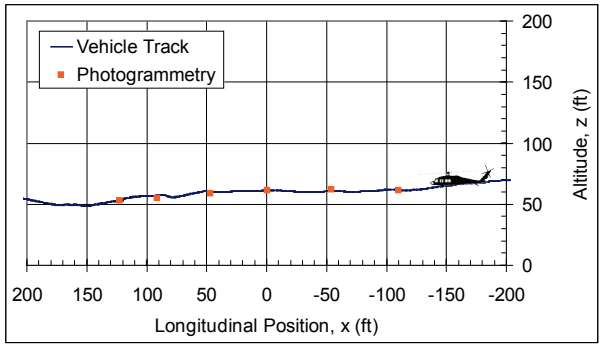

Figure 11. Longitudinal position versus altitude

Photogrammetry Validation - Round Two

For the flight testing done in September, cones were again placed at arbitrary distances in the negative and positive directions along the X and Y axes. The height of the telephone poles could be determined during this test, since all five were contained within the field of view of each camera. The photogrammetry data correlated with physical measurements taken onsite. As the comparison of these values shows in Table 2, the largest magnitude difference is an error of 5.35%, though, in general, measurement accuracy increased.

Table 2. Measured and calculated distances, round two

Object	Measured (ft)	Photogrammetry (ft)	Delta
LZ_0[a] to +X Cone	136.5	136.6	0.08%
LZ_0[a] to -X Cone	153.2	153.1	-0.07%
LZ_0[a] to +Y Cone	75.3	74.4	-1.29%
LZ_0[a] to -Y Cone	79.7	79.0	-0.80%
Pole 1 Height	34*	33.5	-1.57%
Pole 2 Height	34*	33.7	-0.80%
Pole 3 Height	34*	33.5	-1.54%
Pole 4 Height	34*	35.7	4.93%
Pole 5 Height	34*	33.1	-2.53%
UH-1 Tail Height	9.5	10.0	5.35%

[a]Center of Lane 7 in Oasis LZ
*Approximate height

The second method of validation also indicated good agreement between the photogrammetry data and the actual flight track data. Figure 12 shows the longitudinal versus lateral position of the aircraft during the taxi event through Lane 5, with the aircraft traveling approximately 25 kts. The photogrammetry points all fall on the vehicle track. When compared to the vehicle data from the same instant in time, the correlation is also very good. The longitudinal position versus altitude of the aircraft is shown in Figure 13. There is very good agreement between the photogrammetry and the vehicle track near the origin. Variability in the comparison increases slightly toward either extreme.

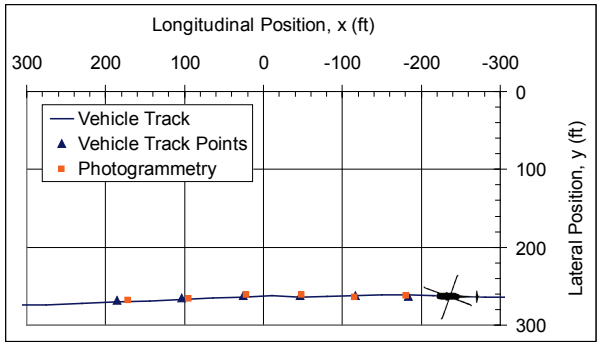

Figure 12. Longitudinal versus lateral position

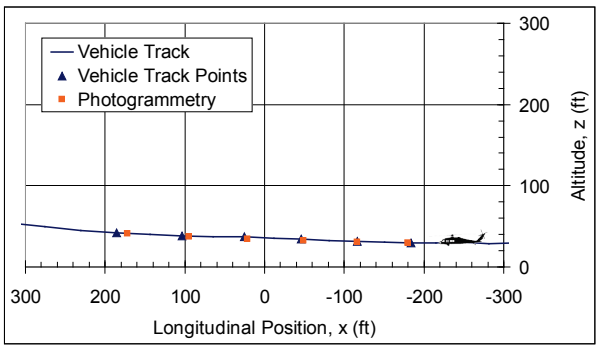

Figure 13. Longitudinal position versus altitude

Brownout Cloud Analysis

Analysis - Round One

Sample brownout cloud data from the first round of flight testing at YPG is found in Figure 14. This figure shows six frames from each of the two cameras at the same instant in time. The 3D view resulting from the photogrammetry process is also shown. In this view, the orange dots are the reference cones (which were imaged before the flights and then removed for the actual flight test), the gray dots are the other reference points, such as the telephone poles and the palm tree, and the blue dots are the aircraft (which is only visible in the final set of images when it exits the brownout cloud). The yellow dots are points on the brownout cloud that could be identified between the two images at the same instant in time. It should be noted, however, that these points do not correlate between image sets. That is, point 27 on the brownout cloud at the first time step does not necessarily correspond to the same point 27 at the next time step. This is due to the large time steps between image sets. Since the goal was to determine if photogrammetry is suitable for brownout cloud measurements, large time steps were used to cover the entire event. Since the data were captured at 15Hz, however, the location of a point on the cloud could be tracked from image set to image set if desired.

Several items stand out when considering the results from the first round of photogrammetry. There was a limited common field of view between the two cameras, which restricted data collection to a very short time duration. Lateral position of the aircraft in the landing lane further complicated this issue. As evidenced in the images, the aircraft is halfway through the frame in the Camera 1 image before it appears in the frame from Camera 2. The positioning of the cameras was optimized for the center of the LZ, inadvertently missing the early cloud formation. With only two views at each time step, shared points in the brownout cloud were difficult to determine. The highly three-dimensional cloud structure further complicates this. Regions of the cloud that are visible in one view are blocked by other regions of the cloud in the other view. The exposure of the images could have been improved as well; the images from Camera 1 are slightly overexposed, while those from Camera 2 are slightly underexposed. The cameras were configured with the same exposure time, but were exposed to dramatically different early-morning sunlight conditions. Even with these limitations, this first round of flight tests clearly proves that photogrammetry is a valid technique for quantitative characterization of brownout cloud events.

Analysis - Round Two

This discussion will focus on three aspects of testing conducted during round two: 1) brownout cloud formation and evolution during a taxi pass, 2) brownout cloud formation and evolution during an approach to touchdown, and 3) chalk dust visualization. Brownout cloud visualization was significantly improved in round two through the use of six high-resolution cameras, as compared to the two, lower-resolution cameras used in round one.

Taxi Pass

During the taxi pass used for validation, the vehicle was low enough that it generated a brownout cloud. This is the same event that was used to obtain the aircraft position plots in Figure 12 and Figure 13. Due to printed space limitations, only one set of six images from this pass is shown (Figure 15). The 3D view resulting from photogrammetry from six different times is shown in Figure 16. As before, the yellow dots represent points on the perimeter of the brownout cloud and the blue dots represent the aircraft.

With the improved setup utilized in round two, significantly greater volumes of data were collected. Increased points of view, image quantity, and resolution provided the ability to characterize the brownout cloud in much more detail. Utilizing this technique, the high three-dimensionality of the brownout cloud is no longer an obstacle to distinguishing features in the cloud. Whereas previously, only five or six points could be accurately identified for each frame, the improved setup raised the number of identifiable points from approximately 50 to over 100.

A top-down view of the LZ and the brownout cloud data is presented in Figure 17. A side view of the same data is shown in Figure 18. In both figures, the aircraft is marked as the spot in the center of the fuselage between the main landing gear wheels. The highly parabolic overall shape of the brownout cloud can be observed in both figures, with the shape of the cloud forming a somewhat tighter parabola as the aircraft progresses through the LZ. The distance at which the aircraft leads the front of the brownout cloud is particularly notable. Initially, this point on the aircraft is about 10 ft ahead of the cloud. As the aircraft travels through Lane 5, that distance increases to around 50 ft with 10 ft of additional altitude gain.

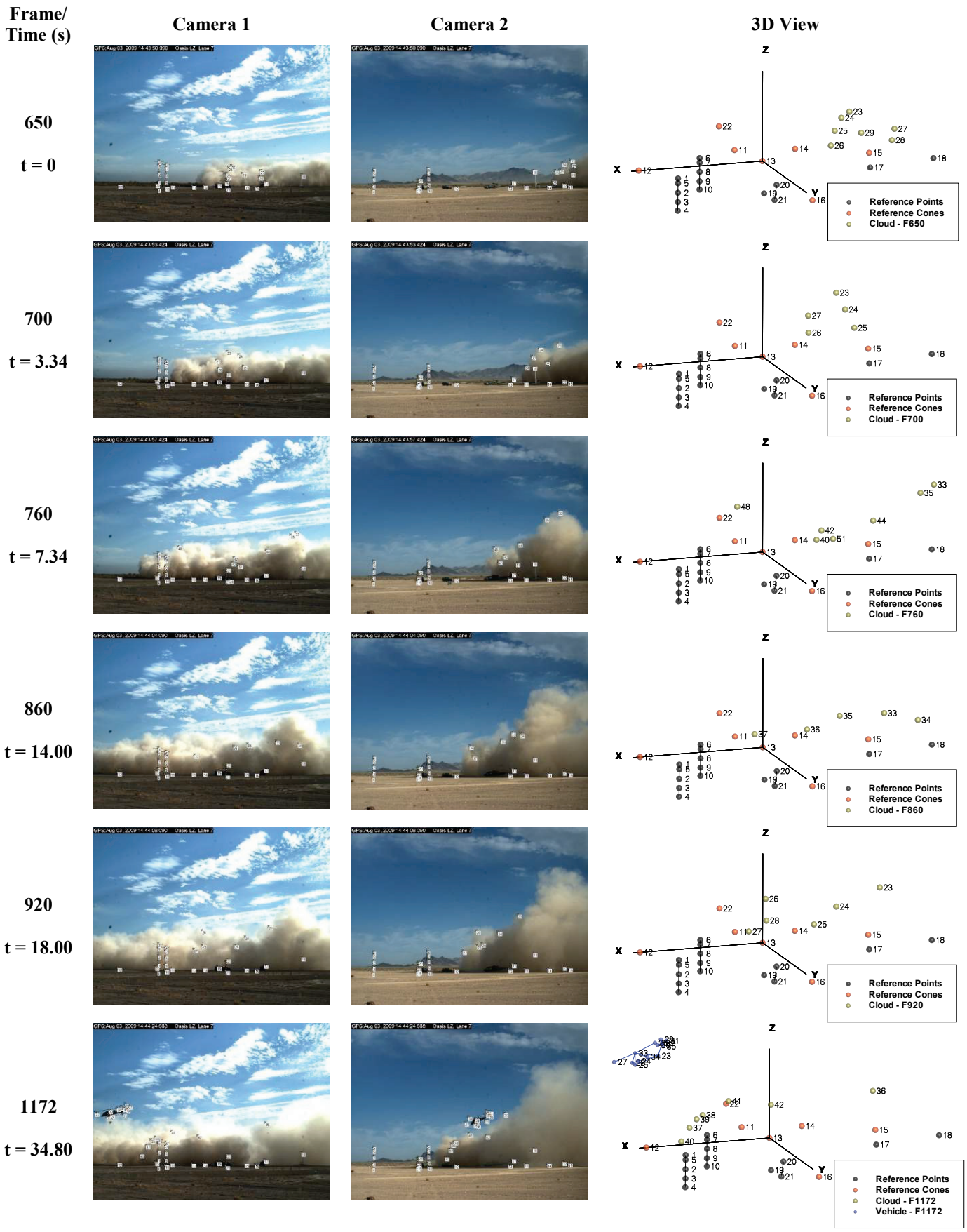

Figure 14. Brownout cloud analysis from first round of testing, Lane 7 approach to touchdown

Camera 1

Camera 2

Camera 3

Camera 4

Camera 5

Camera 6

Figure 15. Brownout cloud analysis from second round of testing, Lane 5 taxi pass images, frame 127, time t = 6.00 s

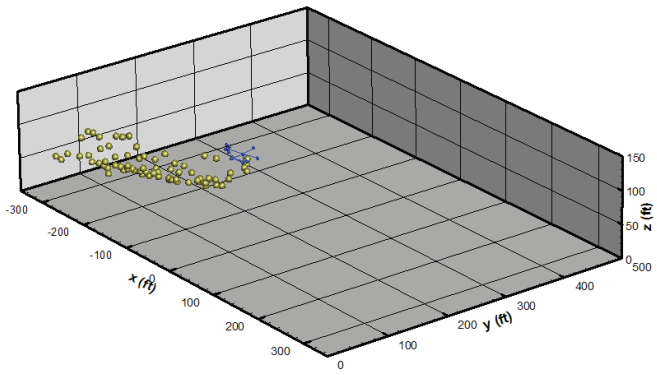

Frame 109/ t = 0 s

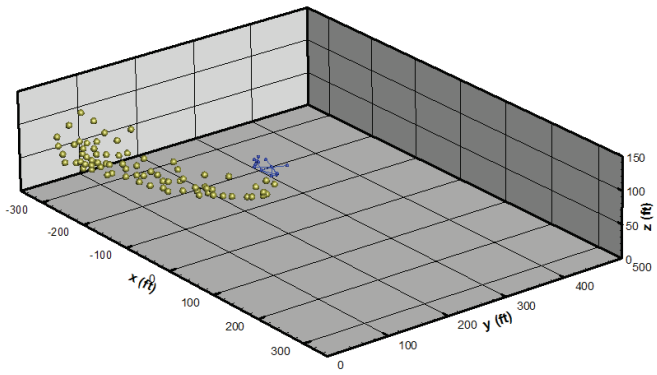

Frame 115/ t = 2.00 s

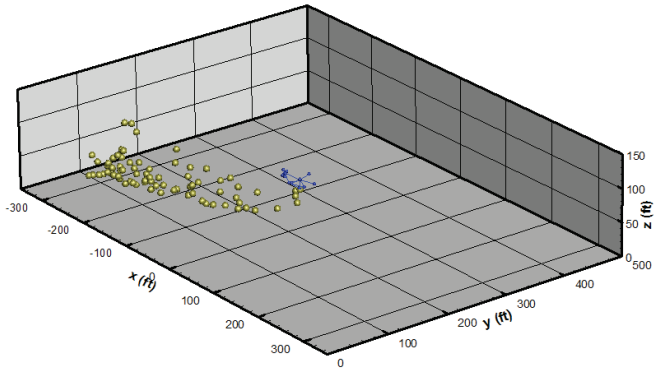

Frame 121/ t = 4.00 s

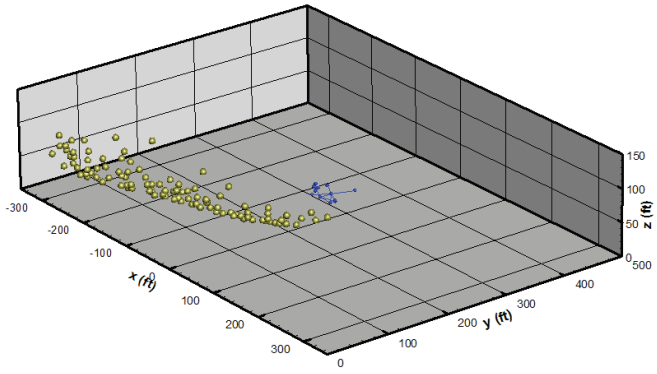

Frame 127/ t = 6.00 s

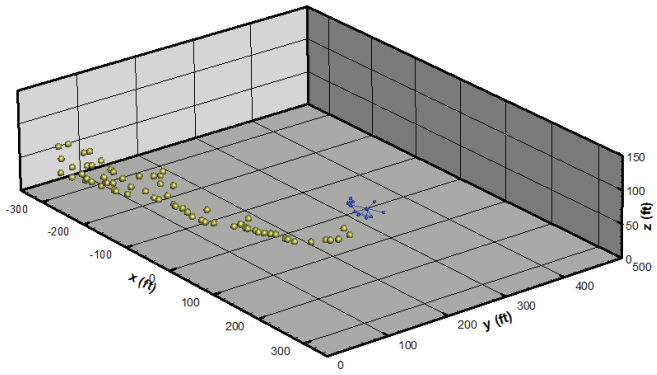

Frame 133/ t = 8.00 s

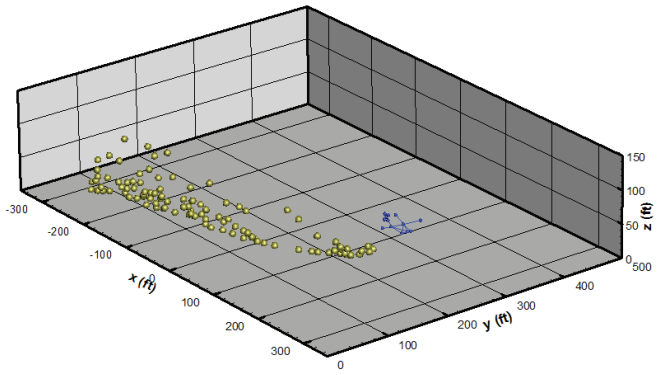

Frame 139/ t = 10.00 s

Figure 16. Brownout cloud analysis from second round of testing, Lane 5 taxi pass 3D views

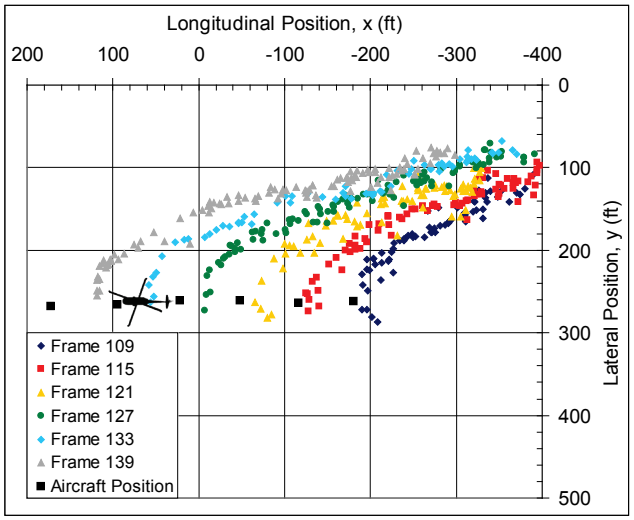

Figure 17. Top-down view of dust cloud progression from Lane 5 taxi

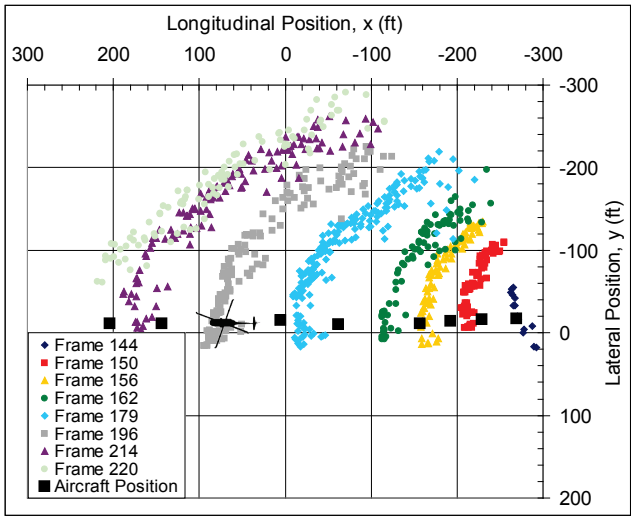

Figure 19. Top-down view of dust cloud progression from Lane 7 approach to touchdown

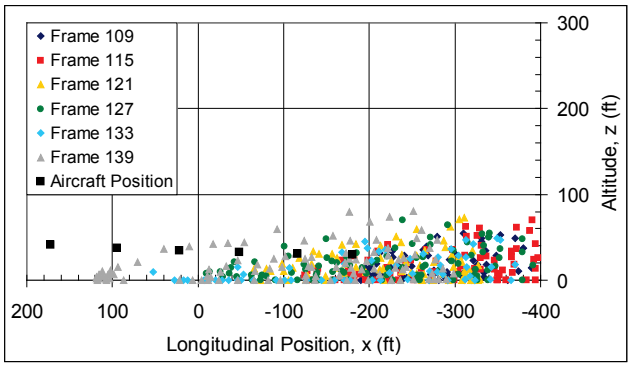

Figure 18. Side view, looking north, of dust cloud progression from Lane 5 taxi

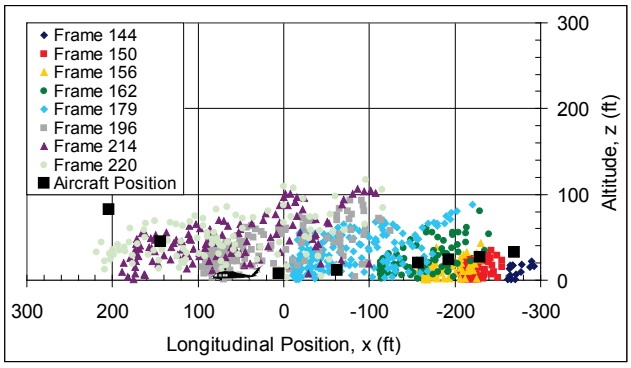

Figure 20. Side view, looking north, of dust cloud progression from Lane 7 approach to touchdown

Approach to Touchdown

The next progression of the analysis was to look at a full brownout approach to touchdown. For illustration, one set of images from one of the eight frames examined of an approach to touchdown event in Lane 7 is shown in Figure 21 on the next page. The resulting 3D views for all eight frames are shown on the page following that in Figure 22.

Top-down and side views of the brownout cloud data are shown in Figure 19 and Figure 20, respectively. In both figures, the image of the aircraft is positioned at approximately the point of touchdown. In the first four frames, the aircraft is visible and its position was determined from photogrammetry. This was also done for the final two frames. In frames 179 and 196, the aircraft is fully engulfed in the brownout cloud. Aircraft position while fully engulfed was determined using onboard data. Comparing the vehicle position to the front of the brownout cloud, it can be seen that the cloud quickly passes ahead of the vehicle. By the third frame, 156, most of the aircraft is surrounded by the cloud. Aside from its expected outward growth, the overall shape of the cloud does not appear to change significantly as time progresses. By the time the aircraft touches down, the cloud has grown to a size between the gray and purple points in the figures. In the final frame, approximately five seconds after takeoff from touchdown , the aircraft has fully exited the cloud.

Chalk Dust Visualization

As described earlier, colored chalk was spread across Lane 7 of the LZ in an attempt to enhance the flow visualization of the brownout cloud. After the initial chalk application, no colored chalk was observed in any of the touchdown events. After that day's testing was complete, the LZ was surveyed. The aircraft touched down in very close proximity to a chalk line on two occasions with little to no chalk being moved or picked up. When the chalk was spread, it was noted that the chalk had a tendency to clump. It is hypothesized that this clumping tendency prevented the chalk from becoming entrained.

For the following day's test, the chalk was mixed with sand from the LZ to more closely approximate the properties of the LZ sand, and was spread across Lane 7 in wider lines, as shown in Figure 23. Chalk entrainment was greatly improved. Red and blue chalk was observed in the brownout cloud, as shown in Figure 24, Figure 25, and Figure 26.

Camera 1

Camera 2

Camera 3

Camera 4

Camera 5

Camera 6

Figure 21. Brownout cloud analysis from second round of testing, Lane 7 approach to touchdown images, frame162, time t = 6.00 s

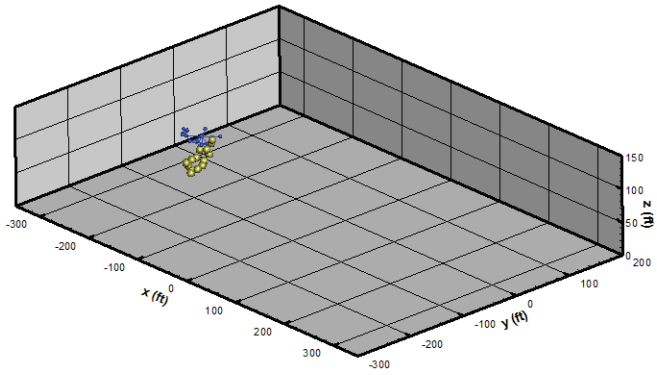

Frame 144/ t = 0 s

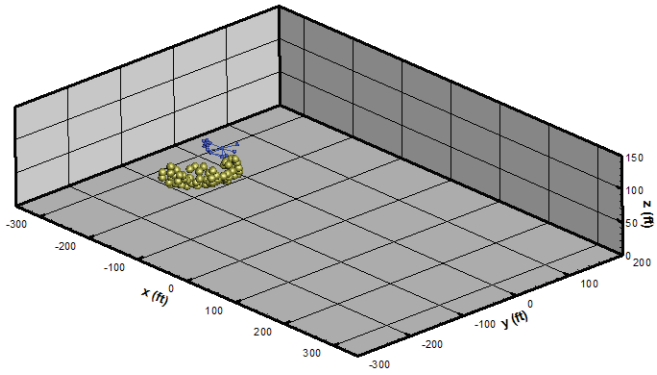

Frame 150/ t = 2.00 s

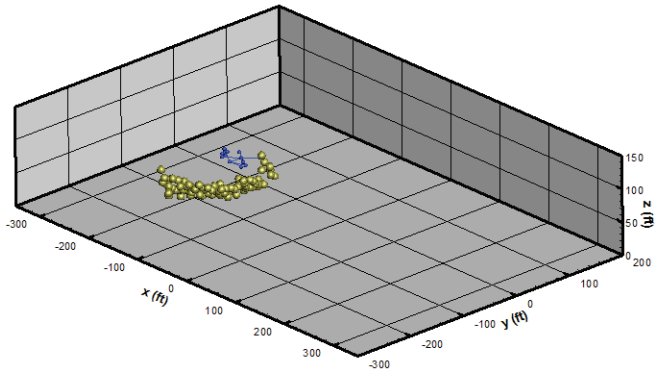

Frame 156/ t = 4.00 s

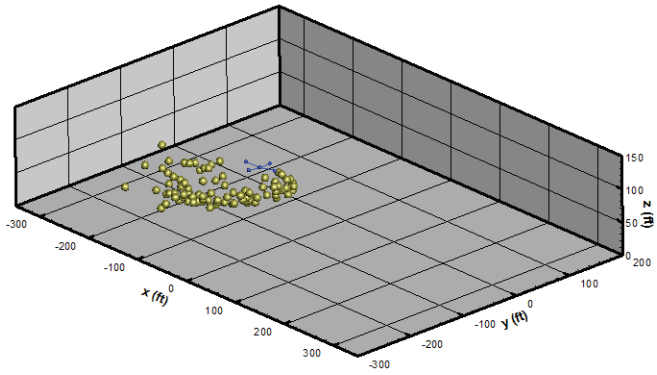

Frame 162/ t = 6.00 s

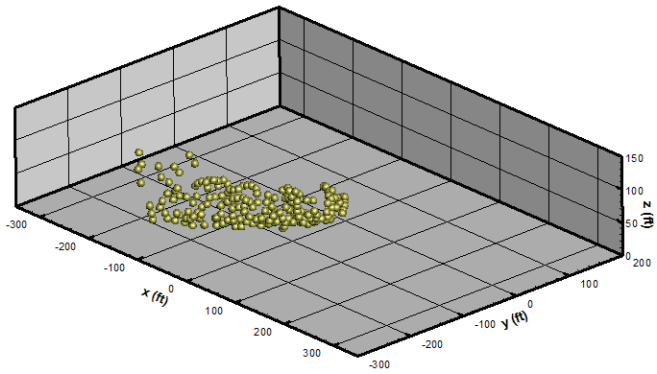

Frame 179/ t = 11.67 s

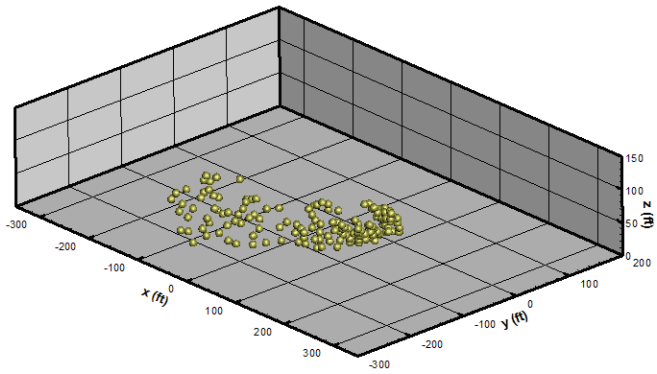

Frame 196/ t = 17.33 s

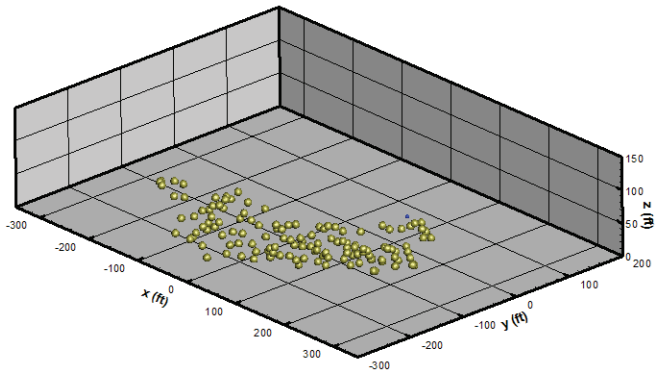

Frame 214/ t = 23.33 s

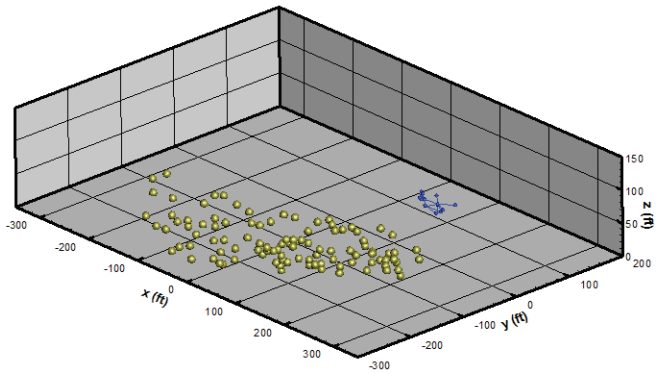

Frame 220/ t = 25.33 s

Figure 22. Brownout cloud analysis from second round of testing, Lane 7 approach to touchdown 3D views

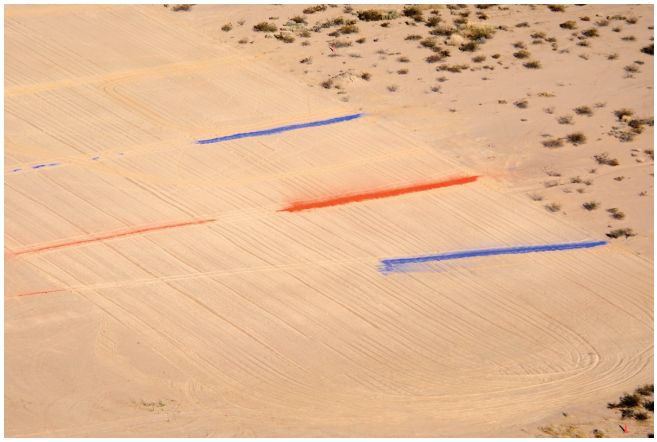

Figure 23. Chalk distribution in Lane 7 on final day of testing

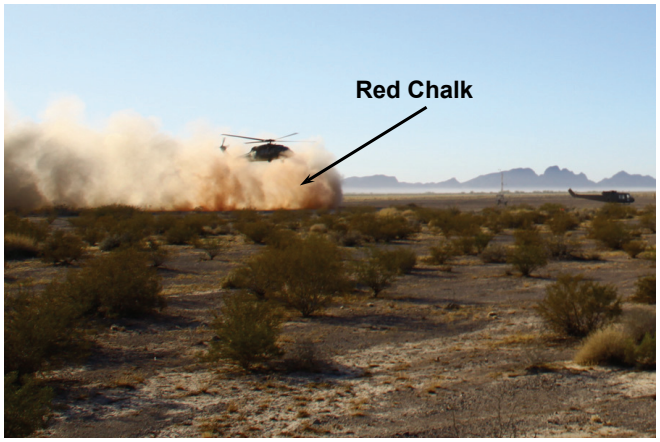

Figure 24. View from Camera 2 of Lane 7 approach to touchdown event with red chalk pickup visible

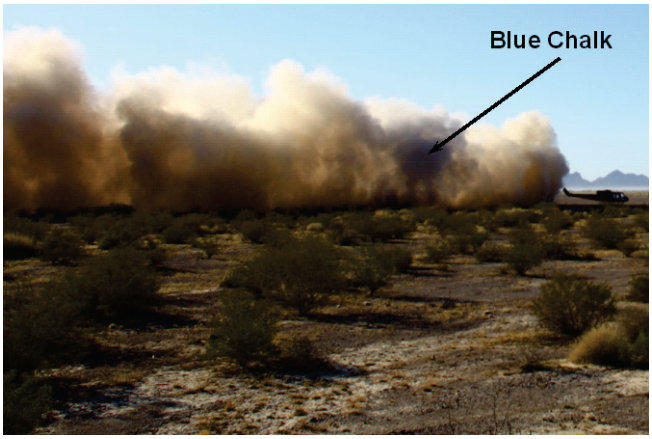

Figure 25. View from Camera 2 of Lane 7 approach to touchdown event with blue chalk pickup visible

Figure 26. View from chase aircraft of EH-60L approach to touchdown in Lane 7

Before and after photographs of the blue chalk line are shown in Figure 27. Prior to inspecting the chalk lines, the research team had hypothesized that all of the chalk would be removed from the surface within one to two landings. Notably, inspection of the chalk lines after testing revealed that this did not happen. While chalk was clearly visible in the brownout cloud, a significant portion of the chalk/sand mixture was in its original position on the ground. This implies that the pickup forces for the cloud are very low. Only the uppermost layer of chalk/sand was removed from the surface during cloud formation.

Figure 27. Blue chalk line 200 ft east of centerline, before and after day two of round two

Conclusions

High resolution flow visualization images of an EH-60L brownout cloud were captured during two rounds of flight tests at the US Army Yuma Proving Ground in southwest Arizona. Photogrammetry was applied and evaluated as a potential technique for quantitative examination of brownout cloud formation and evolution. Two different setups were used to validate the photogrammetry technique. The results of this validation suggest that this process can accurately measure quantitative brownout cloud properties.

Limited success was achieved in the first round of testing. While the technique showed potential, there were significant limitations in the initial photogrammetry setup. These included a small common field of view, poor image contrast due to low sun angle, and the difficulty of visualizing the three dimensional nature of the cloud with only two cameras. These shortcomings were addressed during the second round of flight tests by utilizing an improved system with six higher-resolution cameras.

Quantitative data describing the brownout cloud and its evolution were obtained through images taken during the second round of flight tests with the improved camera system. For the first event investigated, a taxi pass through Lane 5, a greater number of common points were identified on the resulting cloud than before. This allowed the physical size and growth of the cloud to be determined at the six instances in time chosen. The shape of the cloud was parabolic, in both side and top-down views, increasing in tightness as the aircraft progressed through the LZ. It was also noted the rate at which the aircraft, during this taxi pass, appeared to outrun the formation of the cloud. An approach to touchdown event in Lane 7 was also examined, and again the improved setup enabled a much higher resolution of common points on the brownout cloud to be identified. Eight instances in time were investigated for this event, and the size of the cloud was determined at each of these. By the third frame, the majority of the aircraft was surrounded by the cloud, and by the fourth frame two seconds later, the aircraft was completely engulfed in the cloud. Apart from the expected growth of the cloud, its overall shape remained fairly constant throughout the event.

Flow visualization was conducted with lines of chalk dust spread on the LZ. After some refinement, this method showed promise as a seeding technique. It also may provide a mechanism for furthering the understanding of the pickup mechanism of brownout. One of the most significant findings during this portion of the test was that pickup forces of the brownout cloud appear to be very low. This conclusion is based upon the observation that, while chalk was clearly visible throughout the brownout cloud, only a thin layer of the chalk/sand mixture was picked up from the surface of the LZ.

These tests successfully demonstrate that photogrammetry can be utilized as a means for quantitatively observing the formation and evolution of a rotorcraft brownout cloud. Further refinement of the chalk dust flow visualization technique may enable better understanding of the fundamental physics of the brownout cloud particle pickup process. Combined with onboard aircraft data, the resultant data set may validate current and future brownout models and simulations, furthering the understanding of the dangerous phenomenon of brownout.

Acknowledgements

The authors wish to acknowledge the following individuals for their contributions to the success of this endeavor: Walt Harrington, AFRL, for providing the opportunity to participate in these tests; Tom Jones and Benny Lunsford, NASA LaRC, for their expertise and guidance in the development of the photogrammetry system; and Wayne Mantay, AFDD JRPO, for his insight, encouragement, and advocacy.

References

[1] Lee, T.E., Leishman, J.G., and Ramasamy, M., "Fluid Dynamics of Interacting Blade Tip Vortices with a Ground Plane," American Helicopter Society 64th Annual Forum, Montréal, Canada, 29 April – 1 May 2008.

[2] Wachspress, D.A., Whitehouse, G.R., Keller, J.D., Yu, K., Gilmore, P., Dorsett, M., and McClure, K., "A High Fidelity Brownout Model for Real-Time Flight Simulations and Trainers," American Helicopter Society 65th Annual Forum, Grapevine, Texas, 27-29 May 2009.

[3] Phillips, C., and Brown, R.E., "Eulerian Simulation of the Fluid Dynamics of Helicopter Brownout," Journal of Aircraft, Vol. 46, No. 4, pp 1416-1429, July-August 2009.

[4] Buxbaum, P.A., "Landing Makes the Mission," *Special Operations Technology*, Vol. 7, Issue 7, September 2009.

[5] "Sandblaster," *Special Operations Technology*, Vol. 4, Issue 7, October 2006.

[6] Warwick, G., "Brown, Not Out – Helicopter Shoot-Downs in Iraq," *Flight International*, 29 May 2007.

[7] Colby, S., "Military Spin: Help With Brownouts," *Rotor & Wing*, March 2005.

[8] Ryerson, C.C., Haehnel, R.B., Koenig, G.G., and Mouton, M.A., "Visibility Enhancement in Rotorwash Clouds," 43rd AIAA Aerospace Sciences Meeting and Exhibit, Reno, Nevada, AIAA-2005-0263, 10-13 January 2005.

[9] Wadcock, A.J., Ewing, L.A., Solis, E., Potsdam, M., and Rajagopalan, G., "Rotorcraft Downwash Flow Field Study to Understand the Aerodynamics of Helicopter Brownout," American Helicopter Society Southwest Region Technical Specialists' Meeting, Dallas-Fort Worth, Texas, 15-17 October 2008.

[10] Warwick, G., "Dusting Off," *Aviation Week and Space Technology*, 5 May 2008.

[11] Liewer, S., "Desert Landings Rattle Pilots' Nerves," *Stars and Stripes*, 14 April 2003.

[12] Rodgers, S.J., "Evaluation of the Dust Cloud Generated by Helicopter Rotor Downwash," USAAVLABS Technical Report 67-81, March 1968.

[13] Wenren, Y., Walter, J., Fan, M., and Steinhoff, J., "Vorticity Confinement and Advanced Rendering to Compute and Visualize Complex Flows," 44th AIAA Aerospace Sciences Meeting and Exhibit, Reno, Nevada, AIAA-2006-0945, 9-12 January 2006.

[14] Lee, T.E., Leishman, J.G., and Ramasamy, M., "Fluid Dynamics of Interacting Blade Tip Vortices with a Ground Plane," American Helicopter Society 64th Annual Forum, Montréal, Canada, 29 April – 1 May 2008.

[15] Croft, J., "Canadians Demonstrate Brownout Vision Aid," *Flight Global*, 28 April 2009.

[16] Sabbagh, L., "Flying Blind in Iraq: U.S. Helicopters Navigate Real Desert Storms," *Popular Mechanics*, 3 October 2006.

[17] Haehnel, R.B., Moulton, M.A., Wenren, Y., and Steinhoff, J., "A Model to Simulate Rotorcraft-Induced Brownout," American Helicopter Society 64th Annual Forum, Montréal, Canada, 29 April – 1 May 2008.

[18] Phillips, C., and Brown, R.E., "The Effect of Helicopter Configuration on the Fluid Dynamics of Brownout," 34th European Rotorcraft Forum, Liverpool, United Kingdom, 16-19 September 2008.

[19] Wachspress, D.A., Whitehouse, G.R., Keller, J.D., McClure, K., Gilmore, P., and Dorsett, M., "Physics Based Modeling of Helicopter Brownout for Piloted Simulation Applications," Interservice/Industry Training, Simulation and Education Conference (I/ITSEC), Orlando, Florida, No. 8177, 1-4 December 2008.

[20] Johnson, B., Leishman, J.G., and Sydney, A., "Investigation of Sediment Entrainment in Brownout Using High-Speed Particle Image Velocimetry," American Helicopter Society 65th Annual Forum, Grapevine, Texas, 27-29 May 2009.

[21] D'Andrea, A., "Unsteady Numerical Simulations of Helicopters and Tiltrotors Operating in Sandy-Desert Environments," American Helicopter Society Specialists' Conference on Aeromechanics, San Francisco, California, 20-22 January 2010.

[22] Nathan, N.D., and Green, R.B., "Wind Tunnel Investigation of Flow Around a Rotor In Ground Effect," American Helicopter Society Specialists' Conference on Aeromechanics, San Francisco, California, 20-22 January 2010.

[23] Liu, T., Cattafesta, L.N., Radeztsky, R.H., "Photogrammetry Applied to Wind Tunnel Testing," AIAA Journal, Vol. 38, No. 6, pp 964-971, June 2000.

[24] "The Basics of Photogrammetry," Geodetic Services Inc., available from: http://www.geodetic.com/v-stars/info.asp?whatis, accessed 8 February 2010.

[25] Shortis, M.R., Robson, S., Jones, T.W., and Lunsford, C.B., "Parachute Model Validation Using Image Sequences," Eighth Conference on Optical 3-D Measurement Techniques, Zurich, Switzerland, 9-12 July 2007.

[26] Barrows, D.A., "Blade Deformation System Demonstration in NFAC," NASA Fundamental Aeronautics Annual Meeting, Atlanta, Georgia, 7-9 October 2008.

[27] Olson, L.E., Abrego, A.I., Barrows, D.A., and Burner, A.W., "Blade Deflection Measurements of a Full-Scale UH-60A Rotor System," American Helicopter Society Specialists' Conference on Aeromechanics, San Francisco, California, 20-22 January 2010.

[28] Kassander, A.R., and Sims, L.L., "Cloud Photogrammetry with Ground-Located K-17 Aerial Cameras," Journal of Meteorology, Vol. 14, No. 1, pp.43-49, February 1957.

[29] Zehnder, J.A., Zhang, L., Hansford, D., Radzan, A., Selover, N., and Brown, C.M., "Using Digital Cloud Photogrammetry to Characterize the Onset and Transition from Shallow to Deep Convection over Orography," *Monthly Weather Review*, Vol. 134, pp. 2527-2546, September 2006.